THE JOURNAL OF BIOLOGICAL CHEMISTRY VOL. 284, NO. 14, pp. 9280–9289, April 3, 2009

Neurokinin 1 Receptor Mediates Membrane Blebbing in HEK293 Cells through a Rho/Rho-associated Coiled-coil Kinase-dependent Mechanism*[S]

Received for publication, November 20, 2008, and in revised form, January 5, 2009 Published, JBC Papers in Press, January 28, 2009, DOI 10.1074/jbc.M808825200

John Meshki[‡], Steven D. Douglas[‡§], Jian-Ping Lai[‡], Lynnae Schwartz[¶], Laurie E. Kilpatrick[‡§], and Florin Tuluc[‡§1]

From the Divisions of [‡]Allergy and Immunology and [¶]Anesthesiology, Joseph Stokes Jr. Research Institute, The Children's Hospital of Philadelphia, Philadelphia, Pennsylvania 19104 and the [§]Department of Pediatrics, University of Pennsylvania Medical School, Philadelphia, Pennsylvania 19104

We have investigated the effect of neurokinin 1 receptor (NK1R) agonists on HEK293 cells transfected with the NK1R receptor. The NK1R receptor mediates dramatic shape changes that include contractions of the membrane cortex resulting in membrane bleb formation. We have found that the cell shape changes correlate with changes in electrical impedance measured in cellular monolayers. The shape and impedance changes were prevented after preincubation with NK1R antagonists aprepitant and L-73060. Although bleb formation usually heralds apoptotic cell death, we have found that NK1R-mediated cellular blebbing does not associate with apoptosis. Preincubation with a cell-permeable derivative of C3 transferase that blocks Rho or with the Rho-associated coiled-coil kinase inhibitor Y27632 completely prevented NK1R-induced shape and impedance changes. Blebbing was also completely inhibited by ML-9, a myosin light chain kinase inhibitor. Furthermore, the phospholipase C inhibitor U73,122 did not interfere with the effect of Substance P (SP) on cellular morphology and cellular impedance but completely blocked SP-induced intracellular calcium increase, indicating that the blebbing is a process independent of intracellular calcium elevations. Blebbing is a protein kinase C-independent process, since the nonselective protein kinase C inhibitor GF109203X did not interfere with SP-induced effects. Based on these results, we provide the first evidence that NK1R receptor-ligand interaction can cause apoptosis-independent cellular blebbing and that this process is mediated by the Rho/Rho-associated coiled-coil kinase pathway.

Neurokinin 1 receptor (NK1R)[2] mediates a variety of biological effects, including inflammatory processes and immunologic responses (1–6), smooth muscle contraction, hypotensive effects, and stimulation of cellular secretion (7, 8). Two isoforms of NK1R have been described: a full-length NK1R that includes in its primary structure 407 amino acid residues and a truncated NK1R that lacks 96 amino acid residues in the COOH terminus intracellular domain. Both isoforms are functionally active and activated different signaling pathways (9–12). In this study, we have focused on the biology of the full-length NK1R.

It is generally accepted that the NK1R couples mainly to $G_{q/11}$ proteins, resulting in activation of phospholipase C and a transient increase in intracellular inositol 1,4,5-trisphosphate (IP_3) and calcium concentration (13, 14). In addition, NK1R has the ability to induce adenylyl cyclase activation and production of cAMP via the G_s protein, although the potency of the NK1R agonists in generating cAMP accumulation is lower as compared with their ability to induce IP_3 formation and intracellular calcium increase (15). Furthermore, NK1R was also linked to inhibition of adenylyl cyclase production via the pertussis toxin-sensitive G_i protein in rat submandibular cells (16). G protein-independent coupling mechanisms initiated by neurokinin receptors have also been suggested, especially in connection with ion channels (17).

NK1R is an important regulator of motility in a variety of cells. NK1R mediates *in vitro* chemotaxis of human peripheral blood leukocytes (18) and local recruitment of opioid-containing leukocytes in an *in vivo* model of hind paw inflammation in rats (19). Furthermore, the carboxyl-terminal sequence of SP induces chemotaxis of human monocytes (20). SP has chemotactic effect on eosinophils (21); this effect may be at least in part indirect, since it has been found that Substance P stimulates bronchial epithelial cells to release eosinophil chemotactic activity (22). SP stimulates the migration of natural killer cell in a dose-dependent manner, with a maximal response at 10^{-8} M SP (23). Substance P has a role in cancer promotion and progression, through proliferative and antiapoptotic effects (24–26). Additionally, Substance P is a promoter of adult neural progenitor cell proliferation under normal and ischemic conditions (27). SP has a priming effect on undifferentiated THP-1 cells, augmenting the CCR5-mediated calcium increase (9). We have recently shown that SP enhances CCL5-induced chemotaxis of human monocytes (12).

Changes in cellular shape involve cytoskeletal rearrangements resulting in membrane ruffling, extension of filopodia,

* This work was supported, in whole or in part, by National Institutes of Health Grants P01-MH076388 and R01-MH049981 (to S. D. D.). This work was also supported by the Joseph Stokes Jr. Research Institute Foerderer-Murray research award (to F. T.). The costs of publication of this article were defrayed in part by the payment of page charges. This article must therefore be hereby marked "*advertisement*" in accordance with 18 U.S.C. Section 1734 solely to indicate this fact.

[S] The on-line version of this article (available at http://www.jbc.org) contains supplemental Fig. S1.

[1] To whom correspondence should be addressed: 3615 Civic Center Blvd., Abramson Research Bldg., Rm. 1208C, Philadelphia, PA 19104. Tel.: 267-426-5350; Fax: 215-590-3044; E-mail: tuluc@email.chop.edu.

[2] The abbreviations used are: NK1R, neurokinin 1 receptor; IP_3, inositol 1,4,5-trisphosphate; MLC, myosin regulatory light chain; MLCK, myosin regulatory light chain kinase; MLCP, myosin light chain phosphatase; ROCK, Rho-associated coiled-coil kinase; PKC, protein kinase C; Sar9, [Sar^9,$Met(O_2)^{11}$]Substance P; PLC, phospholipase C.

and actin stress fiber formation. Myosin contractility has a central role in cytoskeleton rearrangement, and it is regulated by the phosphorylation of the myosin regulatory light chain (MLC). The phosphorylation state of MLC is held in balance by the two opposing enzymes, myosin regulatory light chain kinase (MLCK) and myosin light chain phosphatase (MLCP). Furthermore, MLC phosphorylation is associated with membrane blebbing (28).

Activation of Rho-associated coiled-coil kinase (ROCK) is associated with increased phosphorylation of MLC by a dual mechanism; activated ROCK directly phosphorylates MLC, and ROCK phosphorylates MLCP, resulting in inhibition of the phosphatase activity (29, 30).

Cell rounding and shrinkage is a result of the actin-myosin cortex contraction and has long been known to be used by cells for detaching and retracting their body during migration. Actin-myosin contraction can also lead to stress on the structural proteins that link cortical actin to the cell membrane, and these proteins can be cleaved. The result is the growth of spherical membrane protrusions, also known as cellular blebs. Bleb formation has been described as a marker of cellular apoptosis and results as a consequence of caspase activation (31, 32). Caspase-3 cleaves the carboxyl-terminal autoinhibitory domain of ROCK, resulting in deregulated and constitutive kinase activity (28). Cell treatment with ROCK inhibitors, including Y27632, results in inhibition of bleb formation without affecting the apoptotic state of the cells (32). Thus, it has been concluded that at least in some cell types, apoptosis occurs independently of blebbing. Furthermore, in recent years it has become evident that membrane blebbing is important in various types of cell movement, cell spreading, and cancer cell invasion (33).

Our study demonstrates that activation of NK1R triggers complex and rapid cellular shape change, including blebbing, in HEK293 cells. This cellular shape change can be quantified using a cellular assay based on electrical impedance measurements in cellular monolayers. NK1R-induced blebbing is not associated with apoptosis, and we have identified the main intracellular signaling mechanisms activated by NK1R that are responsible for Substance P-induced cellular shape change. Cell shape change is dependent on Rho/Rock activation, and it is independent of phospholipase C activation, cytosolic calcium increase, and PKC activation. Based on the known pattern of interactions between other G protein-coupled receptors and the molecular targets that we have investigated, we suggest that NK1R has the ability to interact with proteins from the $G_{12/13}$ family.

EXPERIMENTAL PROCEDURES

Reagents—The plasmid encoding the full-length NK1R was a gift from Dr. Norma Gerard (Harvard University, Boston, MA). The NK1R antagonist, aprepitant (Emend®), manufactured by Merck, was purchased through the Children's Hospital of Philadelphia Pharmacy and purified by chromatography (12). Substance P, [Sar^9,$Met(O_2)^{11}$]Substance P (Sar9), Substance P fragment 4–11, L-73060, and L-73061 were purchased from Sigma. Y27632 was from Biomol (Plymouth Meeting, PA).

Cells—HEK293 cells (human embryonic kidney cells; American Type Culture Collection, Manassas, VA) were grown at 37 °C and 5% CO_2 in 100-mm cell culture dishes (Fisher) in Dulbecco's modified Eagle's medium containing 4.5 g/liter glucose, 584 mg/liter L-glutamine, and 110 mg/liter sodium pyruvate (Mediatech, Manassas, VA), supplemented with 100 units/ml penicillin, 100 μg/ml streptomycin (Invitrogen), and 10% fetal bovine serum (Hyclone, Logan, UT).

Establishment of the NK1R Stable Expressing Cell Lines—NK1R plasmids (full-length NK1R) were transfected into HEK293 cells using Nucleofector (Amaxa, Inc., Gaithersburg, MD) and Cell Line Nucleofection Kit V, according to the manufacturer's instructions. In brief, HEK293 cells (2×10^6 cells) were suspended in 100 μl of Nucleofector solution, and 5 μg of the plasmid encoding NK1R was transfected into HEK293 cells. Transfected cells were transferred to 24-well plates and selected with G418 (1 mg/ml) for 4–6 weeks. The antibiotic-resistant cells were further selected by limited dilution in 96-well plates for another 3–5 weeks. The antibiotic-resistant clones were further selected and characterized by reverse transcription-PCR amplification of NK1R mRNA and flow cytometry assay for surface expression of NK1R (10).

SP-induced Calcium Mobilization in HEK293 Cells—Intracellular calcium measurements were performed in Fura-2-loaded cells using Tsien's ratiometric method (34). Briefly, cells were seeded in 96-well plates and allowed to adhere overnight in a standard cell culture incubator at 37 °C in a humidified atmosphere 5% carbon dioxide and air. Fura-2 loading was performed by incubating cells for 45 min at room temperature in medium containing 4 μM Fura-2/AM and 0.01% Pluronic F-127 (Molecular Probes, Inc., Eugene, OR). Cells were washed in Hanks' balanced salt solution containing 1 mM calcium chloride, and fluorescence was recorded in individual cells using an imaging system from Photon Technologies Inc. (Lawrenceville, NJ). Recordings were performed using excitation wavelengths of 340 and 380 nm, and emitted light was measured at 510 nm. A standardization kit (Molecular Probes) was used to convert the ratio measurements to intracellular calcium concentrations. Peak intracellular calcium increases were determined and used to construct concentration-response curves. Logistic curves were fitted to data and used to derive EC_{50} values for Substance P.

Video Microscopy—Cells were plated in 96-well plates by incubation in complete Dulbecco's modified Eagle's medium at a density of 5,000 cells/well. After 24 h, the medium was replaced with 50 μl of complete Dulbecco's modified Eagle's medium/well. Either 50-μl controls, antagonists, or kinase inhibitors were added at the appropriate times for each antagonist. The agonists were added at a volume of 50 μl/well. The cells were examined on a Olympus CK-X41 microscope. Images were recorded using an Olympus DP-71 camera.

Electron Microscopy—Cells were grown in 6-well plates in complete Dulbecco's modified Eagle's medium, and after 24 h, cell SP (100 nM) or solvent was added to each well. Cells were fixed and subjected to electron microscopy imaging, as previously described (35).

Real Time Cell Electronic Sensing Assay—The real time cell electronic sensing assay is based on electrical impedance readings in cell monolayers plated in wells containing built-in gold electrodes. We have used the analyzer, 16 well e-plates, and the integrated software from Acea Biosciences Inc. (San Diego, CA). Cells were plated at a density of 4,000 cells/well in 100 μl of medium, installed on the analyzer. The analyzer and the installed plates were placed in a standard cell culture incubator, at 37 °C in a humidified atmosphere of 5% carbon dioxide and air. Cells were allowed to adhere to plates overnight. The analyzer was programmed to take readings during the addition of drugs to the medium. Data were recorded and analyzed using the integrated software.

Quantification of Apoptosis by 4′,6-Diamidino-2-phenylindole Staining—Cells were treated for 24 h with the NK1R agonist Sar9 (100 nM), staurosporine (0.5 μM), or solvent (controls) and then were trypsinized, mounted on glass slides, and fixed with 70% ethanol. Cells were then stained for 20 min with 1 mg/ml 4′,6-diamidino-2-phenylindole (Sigma) and examined by fluorescence microscopy. Apoptotic cells were identified by chromatin condensation and fragmentation.

Quantification of Apoptosis by Flow Cytometry—Apoptosis was determined by detecting annexin V binding using flow cytometry. HEK293-NK1R cells were treated with Sar9 (100 nM), staurosporine (0.5 μM), or solvent (controls) for 24 h, and then cells were washed, trypsinized, and then labeled with annexin V-fluorescein isothiocyanate and propidium iodide (5 μg/ml) in staining buffer (containing 1% bovine serum albumin in 50 mmol/liter HEPES buffer, pH 7.4) for 15 min on ice. Fluorescein isothiocyanate-conjugated murine IgG monoclonal antibodies of unrelated specificities were used as controls. After staining, cells were washed in phosphate-buffered saline and fixed in 4% paraformaldehyde prior to flow cytometry assay. Cells were analyzed on a FACScan flow cytometer (BD Biosciences).

Western Blot Analysis—Cells were lysed in LDS sample buffer (Invitrogen) and subjected to sonication using a sonic dismembrator model 100 (Fisher). Cell extracts were subjected to SDS-PAGE and transferred to polyvinylidene difluoride membranes, using the iBlot Gel Transfer System (Invitrogen). After blocking with 5% bovine serum albumin in 0.1% Tween 20, Tris-buffered saline, membranes were incubated with the primary antibody. The following first phosphospecific antibodies were used: anti-MLC2, myosin light chain 2 (Ser^{19}), and anti-MYPT1, myosin-binding subunit of myosin phosphatase (Thr^{853}; Cell Signaling Technology, Beverly, MA). Anti-rabbit horseradish peroxidase (1:3000; Bio-Rad) was used as the secondary antibody. Bands were visualized by enhanced chemiluminescence (Thermo Scientific).

Statistical Analysis—The results are expressed as mean ± S.E. The data were analyzed by Student's *t* test for two group comparisons or analysis of variance for multiple comparisons. Differences were considered significant when p was <0.05. EC_{50} values were obtained by sigmoidal curve fitting using GraphPad Prism 4.0 (GraphPad Software Inc., San Diego, CA).

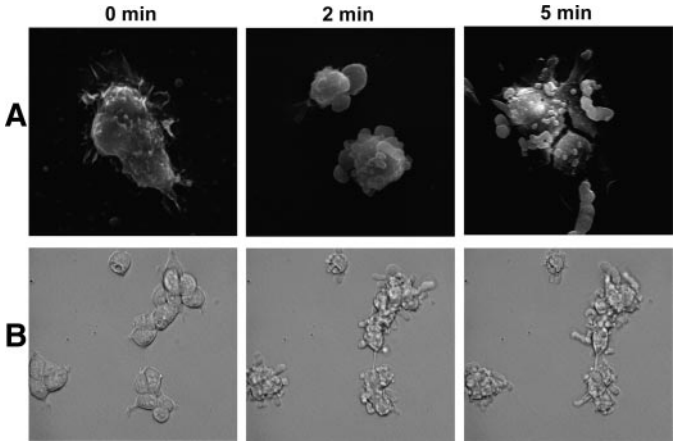

FIGURE 1. **NK1R activation leads to cell shape changes in HEK293 cells.** Scanning electron micrographs (*A*) and phase-contrast micrographs (*B*) of HEK293-NK1R cells treated with 100 nM SP for either 2 or 5 min. Untreated cells (0 min) are shown for comparison.

RESULTS

NK1R Activation Leads to Cell Shape Changes in HEK293-NK1R Cells—Treatment with the NK1R agonist, Substance P, induced dramatic changes in the morphology of HEK293-NK1R cells (Fig. 1). Scanning electron microscopy as well as phase-contrast microscopy revealed both formation of blebs and protrusions emanating from the cell surface. Fig. 1*A* shows scanning electron microscopy of representative cells fixed at 0, 2, and 5 min of stimulation with SP (100 nM). Fig. 1*B* shows time lapse images of cells observed by phase-contrast microscopy. The changes in shape occur at concentrations of SP as low as 0.1 nM, and they start within 1 min of stimulation and last as long as 30 min (supplemental material). The morphological changes persisted for several hours (data not shown).

We quantitated the shape changes in order to calculate EC_{50} values for activation of the NK1R receptor and be able to observe the changes in a less subjective way. By growing cells in plates equipped with electrodes built in the bottom of the wells, we were able to measure the changes in the electric impedance, which measures minute changes in cellular morphology (36). Treatment with varying concentrations of SP reveals a sharp decrease in impedance within the first 2 min (Fig. 2*A*). The changes in impedance were reversible up to 3 nM of SP and reached the maximum amplitude at 100 nM SP. By plotting the decrease in impedance against the concentration of SP, we observed a sigmoidal dose-response curve with an EC_{50} of 1.4 nM (Fig. 2*B*). We compared the changes in impedance to another quantifiable indicator of NK1R activation (*i.e.* mobilization of intracellular calcium). SP caused intracellular calcium increase in a dose-dependent manner (Fig. 2*C*). Plotting the peak changes in calcium against concentrations also shows a sigmoidal dose-response curve with an EC_{50} of 0.1 nM.

Pretreatment of the HEK293-NK1R cells with the NK1R antagonists aprepitant and L-73060 blocked SP-induced intracellular calcium changes, whereas L-73061 (an inactive enantiomer of L-73060) had no effect (Fig. 3*A*). Aprepitant was also able to completely block any changes in impedance caused by SP (Fig. 3*B*). Although L-73060 did not completely block the SP-induced effect on impedance, the response to SP was obvi-

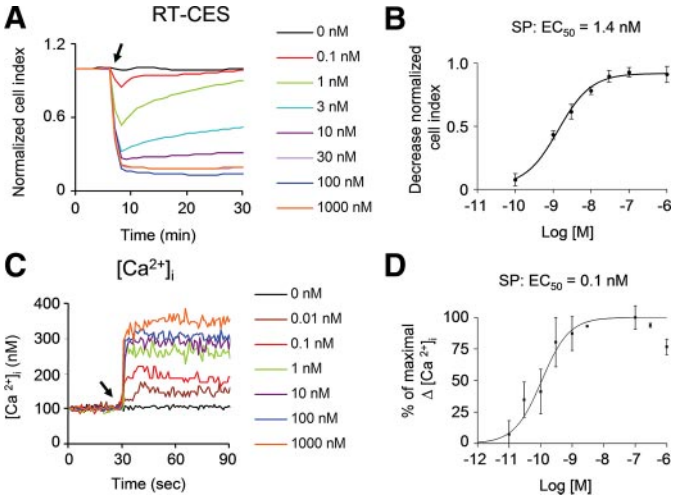

FIGURE 2. **Impedance changes induced by NK1R agonists in HEK293 cells.** *A*, representative real time cell electronic sensor (*RT-CES*) recordings in HEK293-NK1R cells treated with varying doses of SP. SP was added where indicated by an *arrow*. *B*, dose-response curve for the maximum decrease of impedance signal induced by SP in HEK293-NK1R cells. Data were obtained in three independent experiments. *C*, representative tracings of intracellular calcium in HEK293-NK1R cells treated with varying doses of SP, which was added where indicated by an *arrow*. *D*, dose-response curve for the peak intracellular calcium increase induced by SP in HEK293-NK1R cells. Data were obtained from three independent experiments.

ously smaller in cells treated with L-73060 as compared with controls. The inactive enantiomer L-73061 had no effect on SP-induced impedance change (Fig. 3*B*). Phase-contrast microscopy reveals that both of the NK1R inhibitors effectively block the blebbing (Fig. 3, *C* and *D*). No microscopic shape change, intracellular calcium increase, or decrease in impedance values were observed upon SP stimulation of untransfected HEK293 cells or HEK293 cells transfected with the truncated NK1R receptor. These data indicate that the changes in cell shape are a result of activation of the full-length NK1R by Substance P.

Shape Change in HEK293-NK1R Cells Is Not Due to Change in Intracellular Calcium Increase—To determine whether the shape changes induced by SP were due to mobilization of intracellular calcium, we stimulated the HEK293-NK1R cells with ATP. HEK293 cells express endogenous $P2Y_1$ and $P2Y_2$ receptors (37), and they mediate intracellular calcium increase (Fig. 4*A*). Unlike SP, treatment with ATP causes a biphasic response that consists of a brief decrease followed by an obvious increase of impedance measurements, consistent with the cells occupying more area on the plate and spreading out (Fig. 4*B*). The phase-contrast microscopy of the ATP-treated cells shows that the cells did not bleb and they did not contract (Fig. 4*C*).

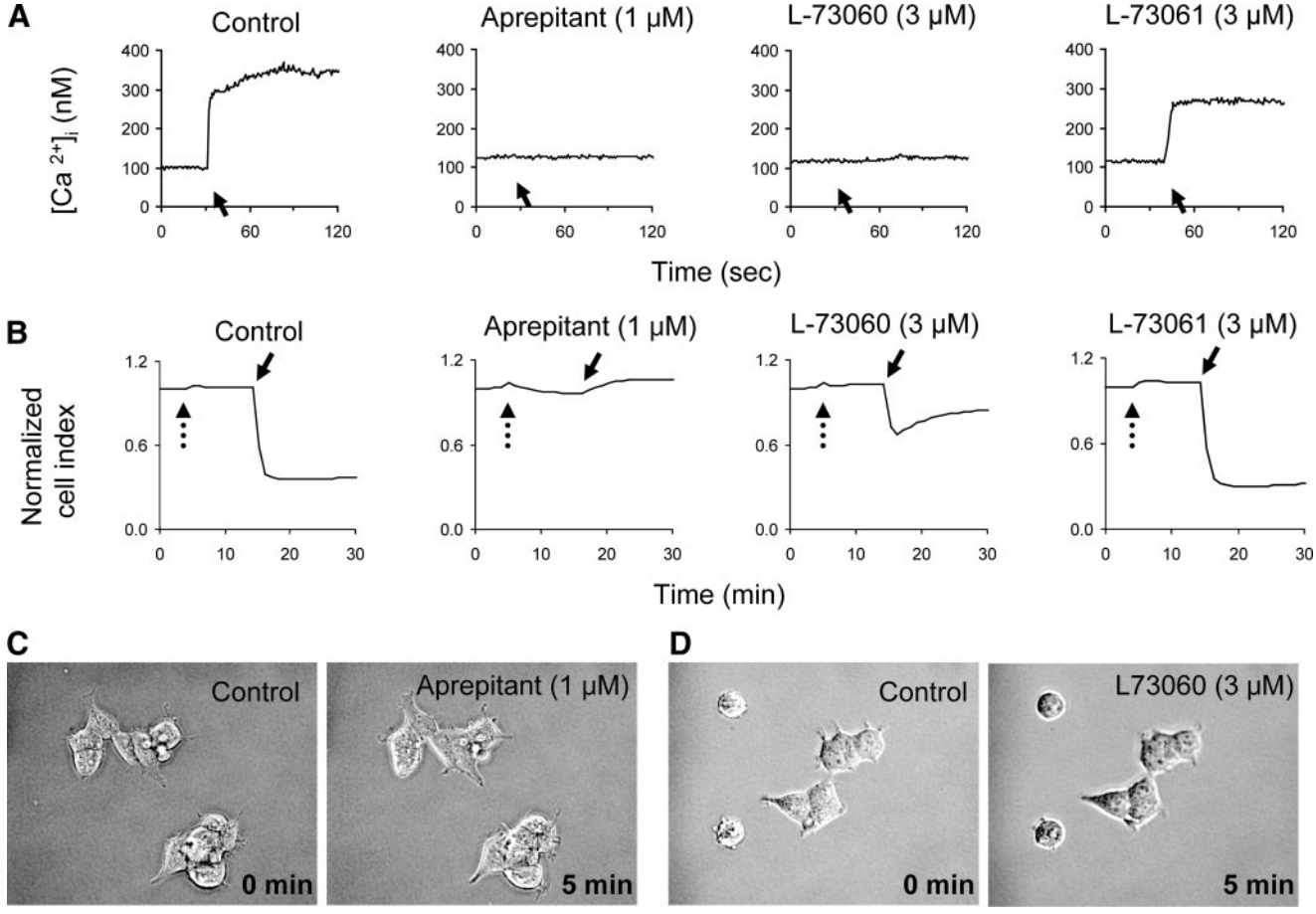

FIGURE 3. **NK1R antagonists block intracellular calcium increase and shape changes.** HEK293-NK1R cells were preincubated with solvent or aprepitant (1 μM), L-73060 (3 μM), or L-73061 (3 μM) for 10 min. *A*, representative intracellular of calcium recordings. SP (100 nM) was added to medium where indicated by *solid arrows*. *B*, representative cell impedance recordings. NK1R antagonists were added where indicated by *dotted arrows*, and SP (100 nM) was added where indicated by *solid arrows*. *C* and *D*, phase-contrast micrographs before (0 min) and 5 min after the addition of SP to cells pretreated with 1 μM aprepitant (*C*) or 3 μM L-73060 (*D*) for 10 min.

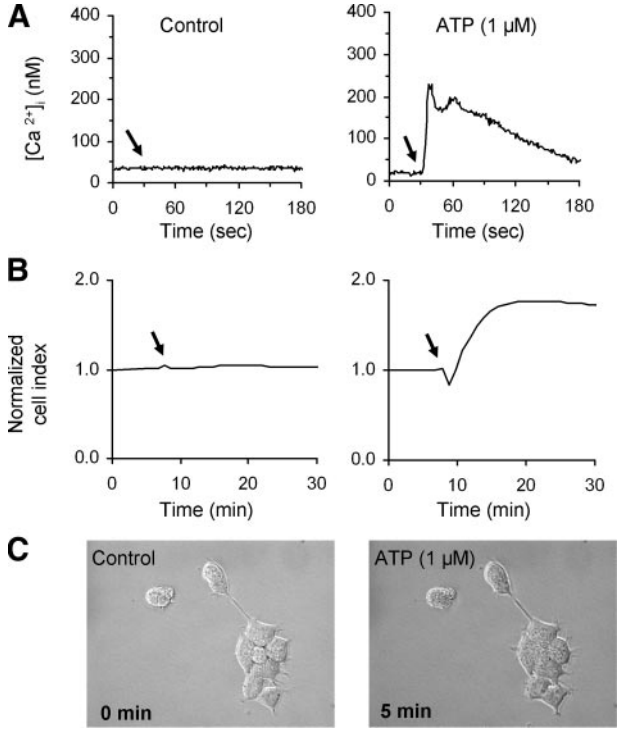

FIGURE 4. **ATP, an agonist at the $P2Y_1$ and $P2Y_2$ receptors, induces impedance changes that are distinct from those mediated by NK1R.** HEK293-NK1R cells were treated with 1 μM ATP. Shown are representative intracellular calcium (*A*) and cell impedance (*B*) recordings in cells treated with ATP (*right*) or solvent (*left*). Reagents were added where indicated by an *arrow*. *C*, phase-contrast micrographs before (0 min) and 5 min after the addition of ATP, showing that ATP does not trigger cell blebbing.

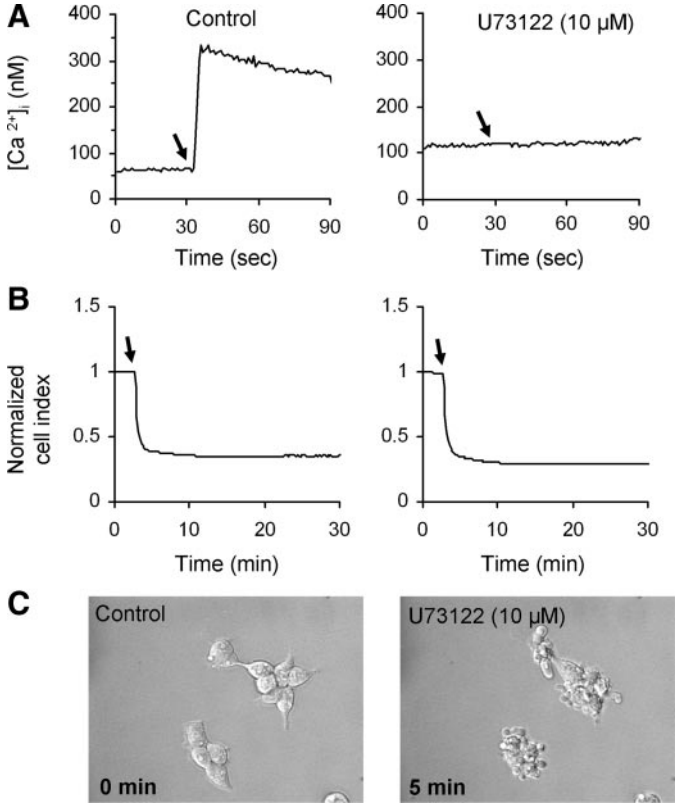

FIGURE 5. **Cellular blebbing induced by NK1R activation is not blocked by the PLC inhibitor U73122.** HEK293-NK1R cells were pretreated with either vehicle or 10 μM U73122 for 30 min, and subsequently, the cells were stimulated with 100 nM SP where indicated by *arrows*. Representative intracellular calcium (*A*) and cell impedance recordings (*B*) in control (*left*) or U73122 (*right*)-treated cells are shown. *C*, phase-contrast micrographs were taken before (0 min) and 5 min after the addition of 100 nM SP.

In order to determine whether activation of phospholipase C plays a role in the shape change induced by SP, we treated HEK293-NK1R cells with the phospholipase C (PLC) inhibitor U73122. Fig. 5*A* shows that the U73122 treatment was sufficient to abolish changes in intracellular calcium. In contrast, there was no effect on the changes in impedance caused by SP in U73122-treated HEK293-NK1R cells (Fig. 5*B*). Also, cell treatment with U73122 did not induce blebbing, and it did not block SP-induced bleb formation and contractions, as visualized by phase-contrast microscopy (Fig. 5*C*).

Implication of Rho/ROCK/MLCK Pathway in HEK293-NK1R Cellular Blebbing—The intracellular mechanisms that are responsible for NK1R-mediated cell shape changes are not known. ROCK has been reported to mediate morphological changes in cells, including bleb formation (31, 32, 38–40). We therefore investigated the consequences of inhibition of ROCK in SP-stimulated HEK293-NK1R cells using a cell-permeable compound, Y27632, which is a highly specific and efficient inhibitor of the ROCK (41). HEK293-NK1R cells treated with Y27632 still displayed calcium mobilization similar to control cells (Fig. 6*A*), but the decrease in impedance values was greatly inhibited (Fig. 6*B*). Furthermore, cell impedance values increased after treatment with SP (Fig. 6*B*), which is most likely due to a tendency of cells to spread more on the substrate (Fig. 6*C*) as well as to the changes in the intracellular ion concentrations (*e.g.* Ca^{2+}) triggered by NK1R activation. Thus, the pretreatment with Y27632 totally abolished blebbing and cell contraction, and in fact some of the cells have undergone spreading on the substrate after treatment with SP.

The effect of Y27632 indicates that ROCK is involved in the shape change of the HEK293-NK1R cells, and because Rho GTPase is a known activator of this protein, we investigated its role in cell NK1R-mediated effects. We used a cell-penetrating form of the *Clostridium botulinum* C3 toxin (C3 transferase) from Cytoskeleton (Denver, CO). The exoenzyme C3 transferase is an ADP ribosyltransferase that selectively ribosylates Rho proteins, rendering them inactive. Pretreatment with the C3 transferase for 24 h had no effect on the calcium mobilization by SP (Fig. 6*A*) but greatly inhibited the SP-induced decrease of impedance values (Fig. 6*B*) and abolished the blebbing and shape changes, as visualized by phase-contrast microscopy (Fig. 6*D*). The MLCK inhibitor ML-9 also inhibited the cellular blebbing (Fig. 6*E*). ML-9 causes massive detachment of cells off of the tissue culture plate, and since impedance measurements requires the cells to be adherent to the plate, impedance measurements were not performed.

PKC Does Not Mediate the Cellular Blebbing/Shape Change—Signaling through the G_q proteins results in activation of classic and novel PKC isoforms as a result of PLC activation and generation of diacyl glycerol from phosphatidylinositol 4,5-bisphosphate. Because the NK1R receptor signals through G_q, we determined whether PKC mediates the shape changes induced by SP. We pretreated cells with the nonselective PKC

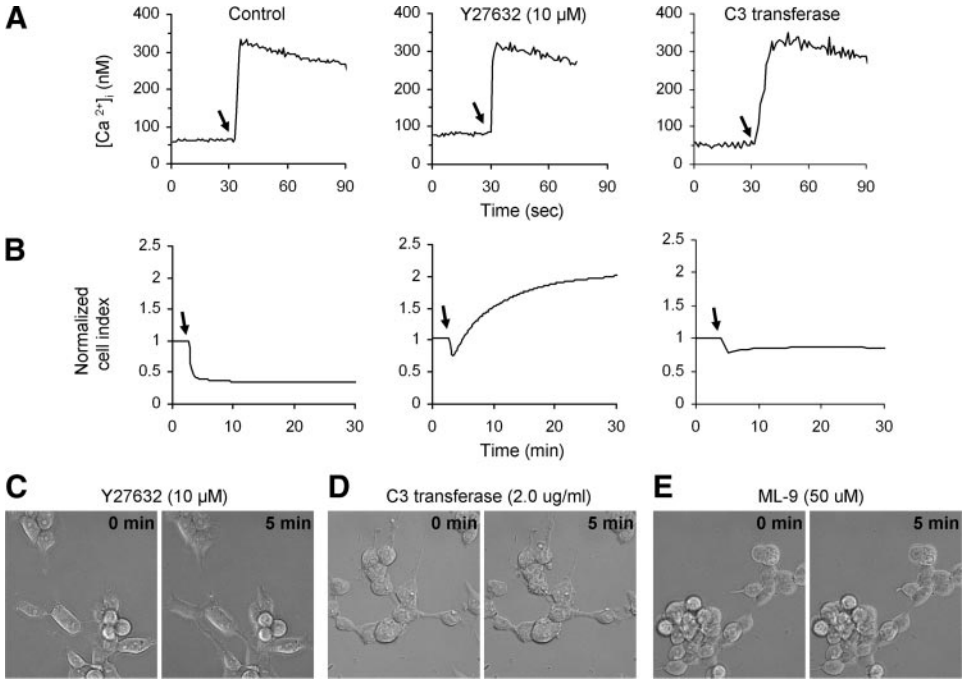

FIGURE 6. **Cellular blebbing induced by NK1R activation is mediated by the ROCK/Rho/MLCK pathway.** *A* and *B*, HEK293-NK1R cells were pretreated with solvent (*left*), 10 μM Y27632 for 1 h (*middle*), or 2.0 μg/ml C3 transferase for 24 h (*right*) and then stimulated with 100 nM SP where indicated by *arrows*. Representative intracellular calcium recordings (*A*) and cell impedance measurements (*B*) are shown. *C–E*, phase-contrast micrographs before (0 min) and 5 min after the addition of 100 nM SP to cells pretreated with 10 μM Y27632 for 1 h (*C*), 2.0 μg/ml C3 transferase for 24 h (*D*), or 50 μM ML-9 for 1 h (*E*).

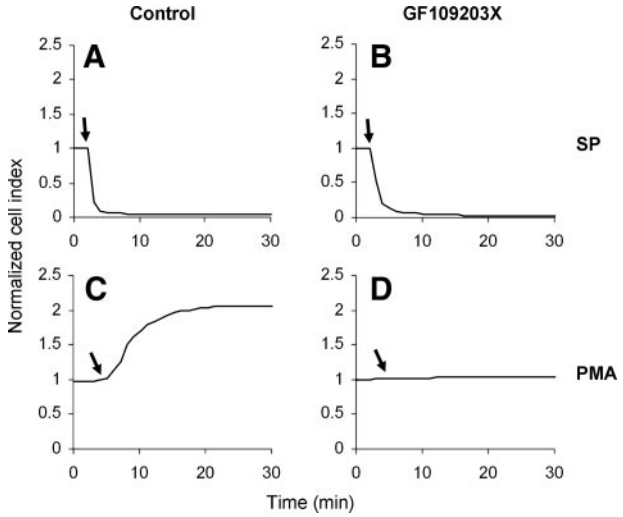

FIGURE 7. **Cellular blebbing induced by NK1R activation is not blocked by the PKC inhibitor GF109203X.** Representative cell impedance measurements of HEK293-NK1R cells pretreated with either vehicle (*A* and *C*) or 5 μM GF109203X (*B* and *D*) for 30 min and then stimulated either with 100 nM SP (*A* and *B*) or 100 nM 12-phorbol 13-myristate acetate (*PMA*) (*C* and *D*).

inhibitor GF109203X. Treatment with the inhibitor had no effect on SP-induced decrease in impedance values (Fig. 7, *top*). To confirm that the treatment with GF109203X resulted in efficient inhibition of PKC, we used 12-phorbol 13-myristate acetate to directly activate PKC. In HEK293 cells, 12-phorbol 13-myristate acetate causes a dramatic increase in impedance, due to a tendency of the cells to spread on the substrate, and this increase was abolished after treating the cells with GF109203X (Fig. 7, *bottom*), confirming that PKC was effectively inhibited.

NK1R-mediated Cellular Blebbing Is Nonapoptotic—Since cellular blebbing is usually associated with apoptosis (31, 32, 42), we investigated if NK1R agonists induce apoptosis in HEK293-NK1R cells. We used Sar9, an endopeptidase-resistant synthetic derivative of SP, to avoid degradation of the agonist during extended incubation with cells. Sar9 is a potent NK1R agonist that induced cell blebbing (data not shown), typical for NK1R receptor activation in this cell type. Cells stimulated with Sar9 (100 nM for 24 h) did not display chromatin condensation and nuclear fragmentation. In parallel experiments, we have treated the cells with staurosporine (0.5 μM for 24 h), which is a well known activator of apoptosis (Fig. 8, *top*). As expected, staurosporine did cause chromatin condensation and nuclear fragmentation. We also measured annexin V binding by flow cytometry as an indicator of apoptosis. The percentages of annexin V-positive cells were 6.3 and 6.5% in control cells and Sar9-stimulated cells, respectively. The percentage of staurosporine-stimulated cells positive for annexin V was 22.8%.

SP Induces MLC and MYPT1 Phosphorylation—MLC phosphorylation on Ser^{19} was examined using a phosphospecific antibody (Fig. 9). SP induced an increase in Ser^{19} phosphorylation after 5 min. NK1R activation caused a significant increase in the levels of MLC phosphorylation. Treatment with the NK1R antagonist aprepitant blocked SP-induced phosphorylation of MLC. We used a cell-permeable derivative of C3 transferase as a Rho inhibitor to investigate the role of Rho on MLC phosphorylation. Inhibition of Rho caused the level of MLC phosphorylation to remain at basal levels when treated with SP. The ROCK inhibitor Y27632 and the MLCK inhibitor caused the levels of MLC phosphorylation to decrease even less than basal levels. These data indicate that MLC phosphorylation can be affected either by blocking activation of the NK1R receptor or inhibiting Rho, ROCK, or MLCK proteins.

We next tested the effects of the inhibitors of cellular blebbing on levels of myosin light chain phosphatase (MLCP) activity. The MLCP holoenzyme includes three distinct subunits: PP1δ, which is the catalytic subunit of the type 1 protein serine/threonine phosphatase family; a 20-kDa small subunit; and a 140-kDa myosin phosphatase targeting/regulatory subunit (MYPT1) (29, 43, 44). Since phosphorylation of MYPT1 on Thr^{696} and Thr^{853} results in phosphatase inhibition, we chose to examine the phosphorylation at the Thr^{853} in MYPT1 using a phosphospecific antibody. SP induced a significant increase in MLCP phosphorylation, whereas treatment with the NK1R antagonist aprepitant blocked this effect. Treatment with the

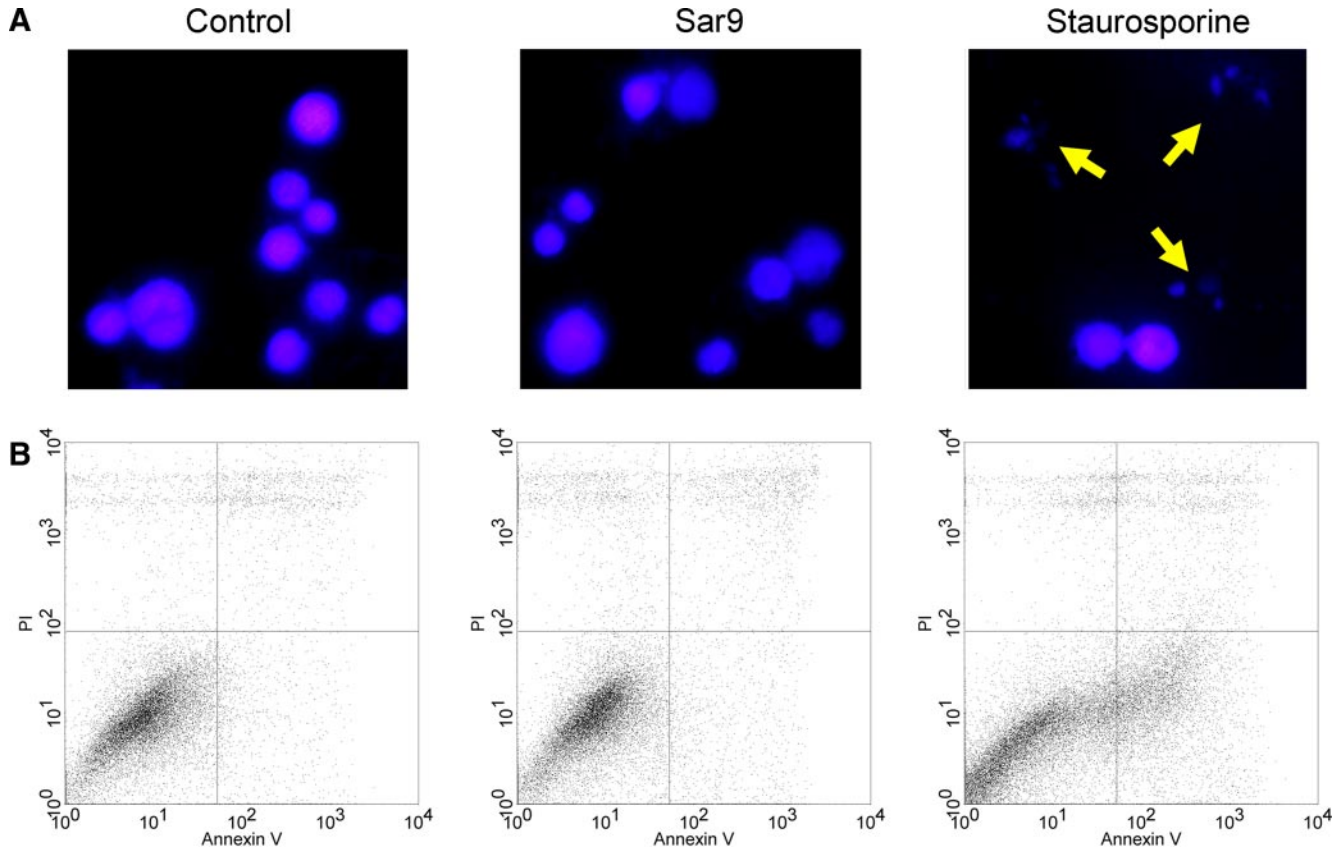

FIGURE 8. **NK1R activation in HEK293 cells does not cause apoptosis.** HEK293-NK1R cells were grown in normal medium for 48 h. Cells were then treated either with vehicle, Sar9 (100 nM), or staurosporine (0.5 μM). Cells were then grown for an additional 24 h and then either subjected to 4′,6-diamidino-2-phenylindole (*DAPI*) staining or flow cytometry analysis. *A*, nuclear morphology is shown 24 h after treatment. Cells were fixed and stained with 4′,6-diamidino-2-phenylindole. *Arrows*, apoptotic cells. *B*, typical fluorescence-activated cell sorting measurement of annexin V (apoptosis marker) and propidium iodide (necrosis marker) 24 h after treatment.

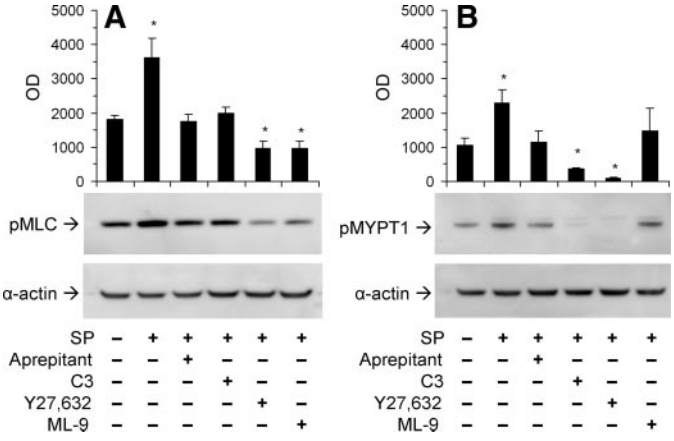

FIGURE 9. **SP-induced MLC and MYPT1 phosphorylation.** Cell lysates were analyzed by Western blotting using primary antibodies directed at phospho-MLC (*A*) or phospho-MYPT1 (*B*). Where indicated, cells were pretreated with solvent (control), C3 tranferase (2.0 μg/ml; 24 h), Y27632 (10 μM; 1 h), or ML-9 (50 μM; 1 h) and then with SP (100 nM; 5 min). Equal protein loading of lanes was confirmed by detecting α-actin. Data are expressed as mean ± S.E. from at least three determinations. *, $p < 0.05$.

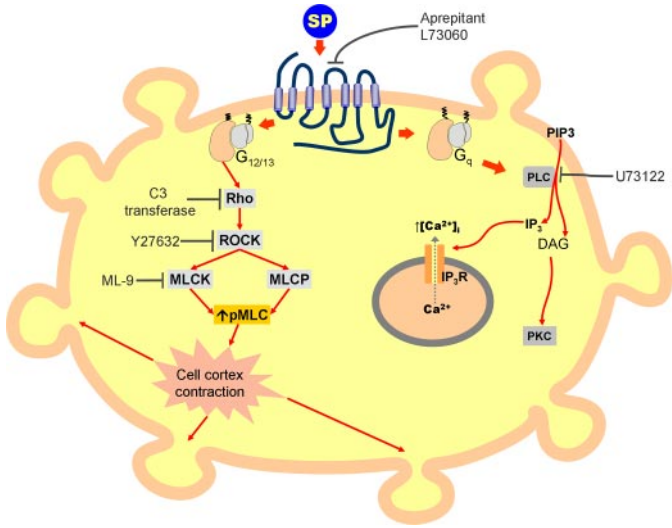

FIGURE 10. **Model for the signaling pathways downstream of NK1R.** Activation of the NK1R receptor by an agonist leads to membrane blebbing. Using U73122 to block the PLC pathway, intracellular calcium mobilization is blocked but membrane blebbing still occurs; therefore, blebbing is initiated before the PLC step, possibly via $G_{12/13}$ proteins. Rho, ROCK, and MLCK are required for NK1R-mediated cell blebbing, as demonstrated using specific inhibitors C3 transferase, Y27632, and ML-9, respectively.

Rho and ROCK inhibitors caused the level of MLCP phosphorylation to decrease as compared with basal levels, whereas treatment with the MLCK inhibitor ML-9 caused no significant change. These data indicate that MLCP phosphorylation can be affected by blocking activation of the NK1R receptor as well as inhibiting the Rho/ROCK pathway.

DISCUSSION

We have shown that activation of the NK1R receptor in HEK293 cells leads to strong and sustained membrane blebbing

as well as membrane protrusions. Electric impedance measurements across a cellular monolayer allowed us to quantitate the changes in cell shape that are attributed to contractions of the membrane cortex, which is composed of an actin and myosin complex with essential functions in maintaining cell shape and in cell locomotion (45, 46). The membrane cortex is structurally connected to the inner face of the lipid-protein mosaic of the membrane through anchoring proteins, such as fodrin (47). Cell membrane blebs form as a result of the contraction of the membrane cortex, which causes the cell to assume a nearly round shape, and when the cortex contraction is excessive, increased hydrostatic pressure develops within the cell. When anchoring proteins of the cortex are disrupted, the hydrostatic pressure pushes the membrane outside, forming blebs. A tightly regulated bleb formation occurs during cell locomotion. We have recently shown that the truncated NK1R modulates CCR5-induced chemotaxis in human monocytes, and it causes potentiation of CCR5-mediated intracellular calcium increase in (12). The mechanism of this regulatory effect is not completely understood. Our present study proves that full-length NK1R can signal through the Rho/ROCK pathway, which is important for cell locomotion (48, 49).

We determined that Substance P-induced blebbing and shape changes are a result of activation of the NK1R receptor by using the NK1R-selective antagonists aprepitant and L-73060. Membrane blebs, cell contraction, and intracellular increases in calcium levels were blocked by NK1R antagonists. In addition, L-73061, the inactive enantiomer of L-73060, had no effect on blebbing, shape change, electric impedance, or calcium mobilization, further confirming that the effect of the NK1R antagonists was specific.

In addition to its well known function as an energy store inside the cell, ATP may escape in the extracellular milieu, where it interacts with membrane receptors that are almost ubiquitously expressed (50, 51). The ability of ATP to induce intracellular calcium changes in HEK293 cells has been attributed to activation of the purinergic receptors $P2Y_1$ and $P2Y_2$ (37). Both of these receptors are known to couple to G_q, resulting in PLC activation and increased intracellular calcium concentrations. ATP does not induce blebbing or cell contraction and in fact leads to spreading of the HEK293 cells on the substrate. Although the endogenously expressed $P2Y_1$ and $P2Y_2$ are not able to mediate blebbing in HEK293 cells, when the P2X7 purinergic receptor is transfected in this cell type, blebbing occurs in response to nucleotide stimulation (52). P2X7-mediated bleb formation requires ROCK activation; however, it should be noted that the $P2X_7$ receptor is not a G protein-coupled receptor, and thus it is not surprising that its signaling mechanisms differ from those triggered by the endogenous $P2Y_1$ and $P2Y_2$ receptors.

Activation of NK1R couples to G_q proteins (14, 53), as well as G_s (15) and G_i and G_z (16, 54). G_q is an important mediator of NK1R activation and leads to activation of PLC that causes phosphatidylinositol 4,5-bisphosphate cleavage to diacylglycerol and IP_3 (53). The release of IP_3 ultimately leads to release of internal stores of calcium. The PLC inhibitor U73122 blocked intracellular calcium increase caused by SP, proving that PLC was effectively inhibited. However, SP-induced blebbing and cell shape change was not affected, suggesting that these effects are independent of the classical G_q pathway involving intracellular calcium increase and PKC activation.

Although differences in signaling mechanisms triggered by NK1R may depend on the cell type, the largest body of evidence suggests that the principal signaling mechanism of NK1R relies on G_q protein and PLC activation. NK1R has been reported to induce adenylyl cyclase activation and production of cAMP via the G_s protein in a Chinese hamster ovary cell line (15); however, NK1R agonists have lower potency in generating cAMP accumulation as compared with their ability to induce IP_3 formation and intracellular calcium increase. Furthermore, we have found that that adenylyl cyclase inhibitor 2′,5′-dideoxyadenosine did not affect SP-induced cell shape and impedance (data not shown).

NK1R triggers inhibition of adenylyl cyclase production via the pertussis toxin-sensitive G_i protein in rat submandibular cells (16), and G_z, which belongs to the G_i family, couples to NK1R in Sf9 cells (54). However, G_i proteins do not play any role in signaling downstream of NK1R in HEK293 cells, because treatment with pertussis toxin, which inhibits G_i proteins, including G_z, had no effect on cell shape change or bleb formation (data not shown).

There are numerous reports on the role of G_{12} and G_{13} in cellular shape changes that have implicated Rho as a mediator downstream of $G_{12/13}$ activation (55–57). Phosphorylation of MLC and activation of the actin-myosin machinery seems necessary for the formation of blebs downstream of NK1R. Rho contributes to MLC phosphorylation, through activation of ROCK (28, 38, 39, 58). The major determinant of MLC phosphorylation is not ROCK, but MLCK, which has an activity that is 1 or 2 orders of magnitude more effective than ROCK in causing MLC phosphorylation (42, 49). Membrane blebbing can occur via caspase cleavage of ROCK in a Rho-independent manner; however, our results demonstrate a critical role for Rho in NK1R-induced blebbing.

Cell treatment with the ROCK inhibitor Y27632 blocked the NK1R-mediated cellular shape change and blebbing. In addition, the cells underwent spreading; this result could be explained by the fact that a basal level of ROCK activation is required for normal cellular integrity, and inhibiting it leads to relaxation of the actin-myosin contractility. ROCK controls the phosphorylation state of MLC through a dual mechanism; on one side, it phosphorylates and activates MLC, and on another side, it inhibits the MLCP.

Blebbing in apoptotic cells results from caspase-mediated activation of ROCK and MLC phosphorylation, acting in a Rho-independent manner. In fact, inhibition of ROCK led to abrogation of cellular blebbing but no other changes in common markers of cellular apoptosis. This is consistent with previous reports showing that SP has an antiapoptotic effect in Kirsten sarcoma virus-transformed rat kidney epithelial cells (25). Our finding led to the conclusion that NK1R-mediated blebbing is not associated with apoptosis, and it is a consequence of Rho-activated ROCK leading to an increase in phosphorylated MLC (Fig. 10). Transfection of cells with dominant negative Rac inhibits MLC phosphorylation (59). We found, however, that inhibition of Rac using NSC23766 (Calbiochem) did not affect

SP-induced cellular blebbing or the levels of MLC phosphorylation (data not shown).

Membrane blebbing also occurs as a consequence of thrombin stimulation in a wortmannin-sensitive manner in CHRF-288 cells (60). Because this effect was shown to act though phosphoinositide 3-kinase, we also tested the effects of wortmannin on SP-induced blebbing and found that it occurred in a phosphatidylinositol 3-kinase-independent manner (data not shown).

Information regarding the mechanisms by which SP binding to the NK1R receptor is translated into signals is limited. We have shown that NK1R mediates dramatic cellular shape changes involving formation of membrane blebs and a drastic reduction of the surface covered by cells. Moreover, we provided evidence that this process is mediated by the Rho/ROCK pathway. Although NK1R agonists trigger a massive intracellular calcium increase in this cell type, our data demonstrate that this process is independent of calcium mobilization or PKC activation. Finally, we present evidence that the membrane blebbing mediated by NK1R is not associated with apoptosis. Thus, we present the first evidence regarding the ability of NK1R to couple to the Rho/ROCK/MLCK pathway, and this will have a significant impact on further characterizing the signaling events initiated by the NK1R.

Acknowledgments—We thank Paula Bruckler for excellent technical assistance, Dr. Glen Rall and Dr. Michal Jarnik (Fox Chase Cancer Center) for the electron microscopy imaging, and Dr. Norma Gerard (Harvard University), for kindly providing the plasmid encoding the NK1R.

REFERENCES

1. Lai, J. P., Douglas, S. D., and Ho, W. Z. (1998) *J. Neuroimmunol.* **86,** 80–86
2. Ho, W. Z., Lai, J. P., Li, Y., and Douglas, S. D. (2002) *FASEB J.* **16,** 616–618
3. Ho, W. Z., Lai, J. P., Zhu, X. H., Uvaydova, M., and Douglas, S. D. (1997) *J. Immunol.* **159,** 5654–5660
4. Guo, C. J., Lai, J. P., Luo, H. M., Douglas, S. D., and Ho, W. Z. (2002) *J. Neuroimmunol.* **131,** 160–167
5. Reed, K. L., Fruin, A. B., Gower, A. C., Stucchi, A. F., Leeman, S. E., and Becker, J. M. (2004) *Proc. Natl. Acad. Sci. U. S. A.* **101,** 9115–9120
6. Weinstock, J. V., Blum, A., Metwali, A., Elliott, D., Bunnett, N., and Arsenescu, R. (2003) *J. Immunol.* **171,** 3762–3767
7. Singh, L. K., Pang, X., Alexacos, N., Letourneau, R., and Theoharides, T. C. (1999) *Brain Behav. Immun.* **13,** 225–239
8. Severini, C., Improta, G., Falconieri-Erspamer, G., Salvadori, S., and Erspamer, V. (2002) *Pharmacol. Rev.* **54,** 285–322
9. Lai, J. P., Ho, W. Z., Kilpatrick, L. E., Wang, X., Tuluc, F., Korchak, H. M., and Douglas, S. D. (2006) *Proc. Natl. Acad. Sci. U. S. A.* **103,** 7771–7776
10. Lai, J. P., Lai, S., Tuluc, F., Tansky, M. F., Kilpatrick, L. E., Leeman, S. E., and Douglas, S. D. (2008) *Proc. Natl. Acad. Sci. U. S. A.* **105,** 12605–12610
11. Fong, T. M., Anderson, S. A., Yu, H., Huang, R. R., and Strader, C. D. (1992) *Mol. Pharmacol.* **41,** 24–30
12. Chernova, I., Lai, J. P., Li, H., Schwartz, L., Tuluc, F., Korchak, H. M., Douglas, S. D., and Kilpatrick, L. E. (2009) *J. Leukocyte Biol.* **85,** 154–164
13. Khawaja, A. M., and Rogers, D. F. (1996) *Int. J. Biochem. Cell Biol.* **28,** 721–738
14. Kwatra, M. M., Schwinn, D. A., Schreurs, J., Blank, J. L., Kim, C. M., Benovic, J. L., Krause, J. E., Caron, M. G., and Lefkowitz, R. J. (1993) *J. Biol. Chem.* **268,** 9161–9164
15. Nakajima, Y., Tsuchida, K., Negishi, M., Ito, S., and Nakanishi, S. (1992) *J. Biol. Chem.* **267,** 2437–2442
16. Laniyonu, A., Sliwinski-Lis, E., and Fleming, N. (1988) *FEBS Lett.* **240,** 186–190
17. Yang, Y. L., Yao, K. H., and Li, Z. W. (2003) *Brain Res.* **991,** 18–25
18. Schratzberger, P., Reinisch, N., Prodinger, W. M., Kahler, C. M., Sitte, B. A., Bellmann, R., Fischer-Colbrie, R., Winkler, H., and Wiedermann, C. J. (1997) *J. Immunol.* **158,** 3895–3901
19. Rittner, H. L., Lux, C., Labuz, D., Mousa, S. A., Schafer, M., Stein, C., and Brack, A. (2007) *Anesthesiology* **107,** 1009–1017
20. Ruff, M. R., Wahl, S. M., and Pert, C. B. (1985) *Peptides* **6,** Suppl. 2, 107–111
21. Dunzendorfer, S., Meierhofer, C., and Wiedermann, C. J. (1998) *J. Leukocyte Biol.* **64,** 828–834
22. Koyama, S., Sato, E., Nomura, H., Kubo, K., Nagai, S., and Izumi, T. (1998) *J. Appl. Physiol.* **84,** 1528–1534
23. Feistritzer, C., Clausen, J., Sturn, D. H., Djanani, A., Gunsilius, E., Wiedermann, C. J., and Kahler, C. M. (2003) *Regul. Pept.* **116,** 119–126
24. Esteban, F., Munoz, M., Gonzalez-Moles, M. A., and Rosso, M. (2006) *Cancer Metastasis Rev.* **25,** 137–145
25. DeFea, K. A., Vaughn, Z. D., O'Bryan, E. M., Nishijima, D., Dery, O., and Bunnett, N. W. (2000) *Proc. Natl. Acad. Sci. U. S. A.* **97,** 11086–11091
26. Amantini, C., Mosca, M., Lucciarini, R., Perfumi, M. C., and Santoni, G. (2008) *J. Pharmacol. Exp. Ther.* **327,** 215–225
27. Park, S. W., Yan, Y. P., Satriotomo, I., Vemuganti, R., and Dempsey, R. J. (2007) *J. Neurosurg.* **107,** 593–599
28. Sebbagh, M., Renvoize, C., Hamelin, J., Riche, N., Bertoglio, J., and Breard, J. (2001) *Nat. Cell Biol.* **3,** 346–352
29. Koga, Y., and Ikebe, M. (2008) *Mol. Biol. Cell* **19,** 1062–1071
30. Eto, M., Kirkbride, J. A., and Brautigan, D. L. (2005) *Cell Motil. Cytoskeleton* **62,** 100–109
31. Coleman, M. L., Sahai, E. A., Yeo, M., Bosch, M., Dewar, A., and Olson, M. F. (2001) *Nat. Cell Biol.* **3,** 339–345
32. Mills, J. C., Stone, N. L., Erhardt, J., and Pittman, R. N. (1998) *J. Cell Biol.* **140,** 627–636
33. Fackler, O. T., and Grosse, R. (2008) *J. Cell Biol.* **181,** 879–884
34. Grynkiewicz, G., Poenie, M., and Tsien, R. Y. (1985) *J. Biol. Chem.* **260,** 3440–3450
35. Gudima, S., He, Y., Meier, A., Chang, J., Chen, R., Jarnik, M., Nicolas, E., Bruss, V., and Taylor, J. (2007) *J. Virol.* **81,** 3608–3617
36. Yu, N., Atienza, J. M., Bernard, J., Blanc, S., Zhu, J., Wang, X., Xu, X., and Abassi, Y. A. (2006) *Anal. Chem.* **78,** 35–43
37. Schachter, J. B., Sromek, S. M., Nicholas, R. A., and Harden, T. K. (1997) *Neuropharmacology* **36,** 1181–1187
38. Gao, S. Y., Li, C. Y., Chen, J., Pan, L., Saito, S., Terashita, T., Saito, K., Miyawaki, K., Shigemoto, K., Mominoki, K., Matsuda, S., and Kobayashi, N. (2004) *Nephron* **97,** e49–e61
39. Leverrier, Y., and Ridley, A. J. (2001) *Nat. Cell Biol.* **3,** E91–E93
40. Paluch, E., Sykes, C., Prost, J., and Bornens, M. (2006) *Trends Cell Biol.* **16,** 5–10
41. Uehata, M., Ishizaki, T., Satoh, H., Ono, T., Kawahara, T., Morishita, T., Tamakawa, H., Yamagami, K., Inui, J., Maekawa, M., and Narumiya, S. (1997) *Nature* **389,** 990–994
42. Totsukawa, G., Wu, Y., Sasaki, Y., Hartshorne, D. J., Yamakita, Y., Yamashiro, S., and Matsumura, F. (2004) *J. Cell Biol.* **164,** 427–439
43. Shimizu, H., Ito, M., Miyahara, M., Ichikawa, K., Okubo, S., Konishi, T., Naka, M., Tanaka, T., Hirano, K., Hartshorne, D. J., *et al.* (1994) *J. Biol. Chem.* **269,** 30407–30411
44. Shirazi, A., Iizuka, K., Fadden, P., Mosse, C., Somlyo, A. P., Somlyo, A. V., and Haystead, T. A. (1994) *J. Biol. Chem.* **269,** 31598–31606
45. Charras, G. T. (2008) *J. Microsc.* (*Oxf.*) **231,** 466–478
46. Charras, G. T., Hu, C. K., Coughlin, M., and Mitchison, T. J. (2006) *J. Cell Biol.* **175,** 477–490
47. Martin, S. J., O'Brien, G. A., Nishioka, W. K., McGahon, A. J., Mahboubi, A., Saido, T. C., and Green, D. R. (1995) *J. Biol. Chem.* **270,** 6425–6428
48. Amano, M., Fukata, Y., and Kaibuchi, K. (2000) *Exp. Cell Res.* **261,** 44–51
49. Amano, M., Ito, M., Kimura, K., Fukata, Y., Chihara, K., Nakano, T., Matsuura, Y., and Kaibuchi, K. (1996) *J. Biol. Chem.* **271,** 20246–20249
50. Williams, M. (1987) *Annu. Rev. Pharmacol. Toxicol.* **27,** 315–345
51. Weisman, G. A., Yu, N., Liao, Z., Gonzalez, F., Erb, L., and Seye, C. I. (2006)

Biotechnol. Genet. Eng. Rev. **22,** 171–195
52. Morelli, A., Chiozzi, P., Chiesa, A., Ferrari, D., Sanz, J. M., Falzoni, S., Pinton, P., Rizzuto, R., Olson, M. F., and Di Virgilio, F. (2003) *Mol. Biol. Cell* **14,** 2655–2664
53. Mizuta, K., Gallos, G., Zhu, D., Mizuta, F., Goubaeva, F., Xu, D., Panettieri, R. A., Jr., Yang, J., and Emala, C. W., Sr. (2008) *Am. J. Physiol.* **294,** L523–L534
54. Barr, A. J., Brass, L. F., and Manning, D. R. (1997) *J. Biol. Chem.* **272,** 2223–2229
55. Bian, D., Mahanivong, C., Yu, J., Frisch, S. M., Pan, Z. K., Ye, R. D., and Huang, S. (2006) *Oncogene* **25,** 2234–2244
56. Nguyen, Q. D., Faivre, S., Bruyneel, E., Rivat, C., Seto, M., Endo, T., Mareel, M., Emami, S., and Gespach, C. (2002) *FASEB J.* **16,** 565–576
57. Kurose, H. (2003) *Life Sci.* **74,** 155–161
58. Riddick, N., Ohtani, K., and Surks, H. K. (2008) *J. Cell. Biochem.* **103,** 1158–1170
59. Gutjahr, M. C., Rossy, J., and Niggli, V. (2005) *Exp. Cell Res.* **308,** 422–438
60. Vemuri, G. S., Zhang, J., Huang, R., Keen, J. H., and Rittenhouse, S. E. (1996) *Biochem. J.* **314,** 805–810